

# LRRC31 is induced by IL-13 and regulates kallikrein expression and barrier function in the esophageal epithelium

RJ D'Mello<sup>1</sup>, JM Caldwell<sup>1</sup>, NP Azouz<sup>1</sup>, T Wen<sup>1</sup>, JD Sherrill<sup>1</sup>, SP Hogan<sup>1</sup> and ME Rothenberg<sup>1</sup>

Eosinophilic esophagitis (EoE) is an allergic inflammatory disease of the esophagus featuring increased esophageal interleukin-13 (IL-13) levels and impaired barrier function. Herein, we investigated leucine-rich repeat-containing protein 31 (LRRC31) in human EoE esophageal tissue and IL-13-treated esophageal epithelial cells. *LRRC31* had basal mRNA expression in colonic and airway mucosal epithelium. Esophageal *LRRC31* mRNA and protein increased in active EoE and strongly correlated with esophageal eosinophilia and *IL13* and *CCL26* (chemokine (C–C motif) ligand 26) mRNA expression. IL-13 treatment increased *LRRC31* mRNA and protein in air–liquid interface-differentiated esophageal epithelial cells (EPC2s). At baseline, differentiated LRRC31-overexpressing EPC2s had increased barrier function (1.9-fold increase in transepithelial electrical resistance ( $P < 0.05$ ) and 2.8-fold decrease in paracellular flux ( $P < 0.05$ )). RNA sequencing analysis of differentiated LRRC31-overexpressing EPC2s identified 38 dysregulated genes ( $P < 0.05$ ), including five kallikrein (KLK) serine proteases. Notably, differentiated LRRC31-overexpressing EPC2s had decreased KLK expression and activity, whereas IL-13-treated, differentiated *LRRC31* gene-silenced EPC2s had increased KLK expression and suprabasal epithelial detachment. We identified similarly dysregulated KLK expression in the esophagus of patients with active EoE and in IL-13-treated esophageal epithelial cells. We propose that LRRC31 is induced by IL-13 and modulates epithelial barrier function, potentially through KLK regulation.

## INTRODUCTION

Eosinophilic esophagitis (EoE) is a chronic disease of the esophagus that has emerged over the past two decades as a unique and complex clinicopathologic condition associated with esophageal dysfunction.<sup>1</sup> The disease is driven by T helper type 2 immune responses to food antigens, and recent genetic and genome-wide association studies suggest that the esophageal epithelium has a critical function in EoE pathogenesis.<sup>2–5</sup> Anatomically, the lumen of the esophagus is lined with non-keratinized stratified squamous epithelium that is made of three layers, organized from the esophageal lumen to the basement membrane as the stratum corneum (SC), the stratum spinosum, and the stratum germinativum (SG).<sup>6</sup> In EoE, esophageal tissue has disorganized epithelium with loss of the SC, expansion of the SG, and impaired barrier function (IBF), demonstrated by decreased transepithelial electrical resistance

(TER) and increased small-molecule paracellular flux.<sup>7</sup> IBF is at least partially caused by the effects of interleukin-13 (IL-13) on esophageal epithelial cells.<sup>3</sup> IL-13, which is highly upregulated in esophageal tissue of patients with EoE, is sufficient to promote IBF in differentiated esophageal epithelial cells (EPC2s) grown at the air–liquid interface (ALI).<sup>3,7–9</sup> Interestingly, desmoglein-1 (DSG1) is downregulated by IL-13 treatment of these cells and in the esophagus of patients with EoE.<sup>7,10</sup> Gene silencing of DSG1 in differentiated EPC2s is sufficient to induce IBF, although not to the extent of that induced by IL-13 treatment. Furthermore, IL-13 is sufficient to alter gene expression of esophageal epithelial cells *in vitro*, and these changes significantly overlap with the transcriptional changes observed in the esophagus of patients with EoE, including downregulation of epidermal differentiation complex genes.<sup>9,11</sup> Notably, mutations in epidermal differentiation

<sup>1</sup>Division of Allergy and Immunology, Department of Pediatrics, Cincinnati Children's Hospital Medical Center, Cincinnati, Ohio, USA. Correspondence: M Rothenberg (Rothenberg@cchmc.org)

Received 21 May 2015; accepted 27 July 2015; published online 14 October 2015. doi:10.1038/mi.2015.98

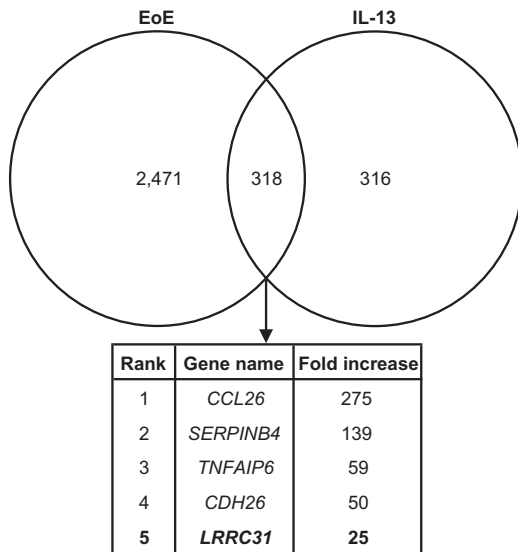


**Figure 1** Identification of leucine-rich repeat-containing protein 31 (*LRR31*). Venn diagram depicting genes differentially expressed  $\geq 1.5$ -fold in the esophagus in eosinophilic esophagitis (EoE) (2,789 genes) and in interleukin-13 (IL-13)-treated esophageal epithelial cells (634 genes) by microarray gene expression analysis. Genes overlapping between these two data sets were identified (318 genes). *LRR31* is in bold and was increased 25-fold.

complex genes are associated with diseases involving IBF in the skin, a tissue that has a similar mucosal structure to the esophagus.<sup>3</sup>

Within the skin, barrier function is maintained in the SC by the cornified cell envelope, which is composed of proteins and lipids that provide mechanical strength and form a hydrophobic barrier, and corneodesmosomes, which are made up of cadherins, DSG1, and desmocollins.<sup>12</sup> The cornified cell envelope and corneodesmosomes are partially regulated by tissue kallikreins (KLKs), serine proteases that cleave filaggrin (FLG), DSG1, desmocollins, and other molecules required for normal barrier formation.<sup>12,13</sup> Genetic mutations in *FLG* and KLK inhibitors, such as serine peptidase inhibitor Kazal-type 5, cause barrier defects in the skin of patients with atopic dermatitis.<sup>12</sup> Interestingly, nearly 50% of patients with EoE have concurrent or past atopic dermatitis.<sup>3</sup> However, the expression and function of KLKs has not been investigated in the esophageal epithelium or in EoE. Herein, we report that leucine-rich repeat-containing protein 31 (*LRR31*) regulates esophageal epithelial barrier function, at least in part by modulating the expression and activity of KLKs.

## RESULTS

### Identification of *LRR31*

We identified 2,789 genes that were differentially expressed  $\geq 1.5$ -fold in EoE ( $P < 0.05$ ) and 634 genes that were differentially expressed  $\geq 1.5$ -fold in IL-13-treated primary esophageal epithelial cells ( $P < 0.05$ ) by microarray gene expression analysis. Comparing these two sets of differentially expressed genes, we identified *LRR31* as one of the most

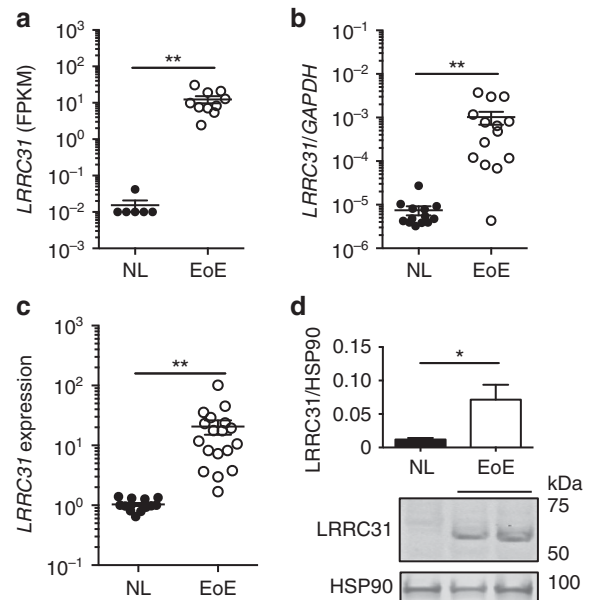


**Figure 2** Leucine-rich repeat-containing protein 31 (*LRR31*) expression in the esophagus. (a) *LRR31* mRNA expression in esophageal biopsies of 16 subjects (6 normal controls (NL), 10 active eosinophilic esophagitis (EoE)) as determined by RNA sequencing analysis. (b) Normalized *LRR31* mRNA expression in esophageal biopsies (13 NL, 14 EoE) as determined by quantitative PCR (qPCR) analysis. (c) Normalized *LRR31* mRNA expression in esophageal biopsies (14 NL, 18 EoE) as determined by microarray gene expression analysis. (d) *LRR31* (61.5 kDa) protein expression in esophageal biopsies (12 NL, 13 EoE) as determined by western blot analysis. Image shown is a representative experiment; heat-shock protein 90 (HSP90) (90 kDa) loading control is shown. Expression level of *LRR31* protein was quantified and normalized to the level of HSP90 protein (mean normalized signal of all patients are graphed). For (a–c), data points represent individual subjects. For (a–d), data are represented as the mean  $\pm$  s.e.m. \* $P < 0.05$  and \*\* $P < 0.01$ .

highly upregulated genes in the esophagus of patients with active EoE and in IL-13-treated primary esophageal epithelial cells (Figure 1).<sup>9,11</sup>

### *LRR31* is specifically induced in EoE

RNA sequencing of esophageal biopsies from control patients (NL;  $n = 6$ ) and patients with active EoE ( $n = 10$ ) showed an EoE-specific 808-fold increase ( $P < 0.01$ ) in *LRR31* mRNA expression (Figure 2a). In an additional cohort, quantitative PCR (qPCR) detected a 137-fold increase ( $P < 0.01$ ) in esophageal *LRR31* mRNA expression in patients with active EoE ( $n = 14$ ) compared with that in NL ( $n = 14$ ) (Figure 2b). We found that *LRR31* mRNA expression increased 18-fold ( $P < 0.05$ ) in patients with active EoE ( $n = 18$ ) compared with NL ( $n = 14$ ) as determined by microarray gene expression analysis (Figure 2c). Western blot analysis showed that *LRR31* protein was readily detectable in active EoE patient esophageal tissue and increased sixfold ( $P < 0.05$ ) in active EoE compared with NL patient esophageal tissue (Figure 2d). These cumulative data indicate upregulation of *LRR31* mRNA and protein expression occurs in the esophagus of patients with active EoE.

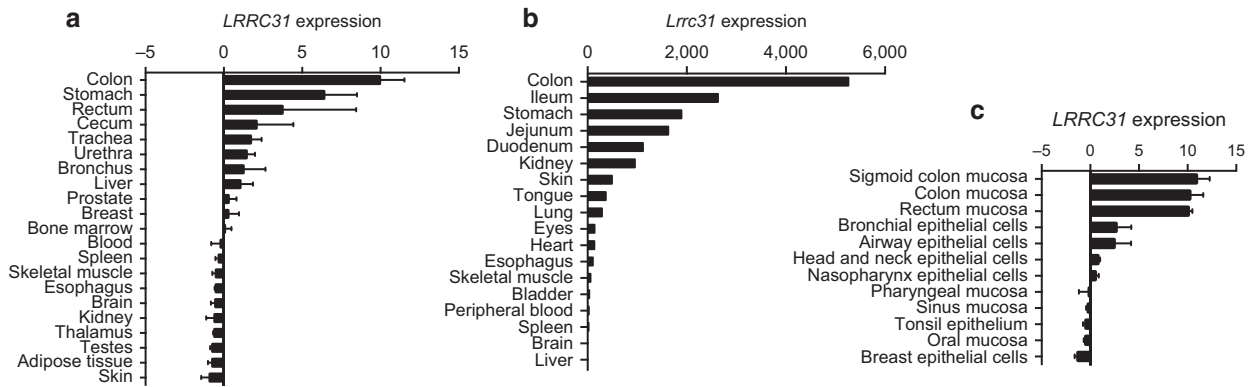


**Figure 3** Expression of leucine-rich repeat-containing protein 31 (*LRRC31*) in human and murine tissue. (a) Normalized *LRRC31* mRNA expression in various normal human tissues as determined by microarray expression analysis. Data from GeneAtlas microarray data set.<sup>14,15</sup> (b) Normalized *Lrrc31* mRNA expression in various normal murine tissues (C57BL/6) as determined by qPCR analysis. (c) Normalized *LRRC31* mRNA expression in healthy human mucosal epithelium and epithelial cell lines as determined by microarray expression analysis. Data from Barcode on Normal Tissue microarray data set.<sup>14,15</sup> For (a, c), data are represented as the mean  $\pm$  s.e.m.

### LRRC31 is expressed in the colon and mucosal tissue

Interestingly, microarray gene expression analysis of a spectrum of human tissues derived from healthy controls retrieved from BioGPS.org revealed that the colon had the highest expression levels of *LRRC31* mRNA, whereas the esophagus did not express detectable levels of *LRRC31* mRNA under homeostatic conditions (Figure 3a).<sup>14,15</sup> qPCR analysis of *LRRC31* mRNA in C57BL/6 murine tissue exhibited a similar pattern of expression, with the colon having the highest mRNA expression and the esophagus having no detectable mRNA expression under homeostatic conditions (Figure 3b). An additional survey of microarray gene expression data from more specific human tissue compartments retrieved from BioGPS.org identified that mucosal epithelia showed the highest *LRRC31* mRNA expression, specifically the mucosal epithelium of the large intestine and bronchial and airway epithelial cells (Figure 3c).<sup>14,15</sup> Collectively, these data suggest that *LRRC31* mRNA displays a conserved pattern of homeostatic expression, in that it is highly expressed in the mucosal epithelium of the colon and lung, and not expressed in the esophagus.

### LRRC31 expression parallels disease activity

EoE cases were stratified by responsiveness to topical fluticasone propionate (FP), a glucocorticoid that has been shown to be effective in controlling disease activity, and to diet therapy. *LRRC31* mRNA expression decreased 17-fold ( $P < 0.01$ ) in FP-responsive cases ( $n = 14$ ) but remained increased 32-fold ( $P < 0.001$ ) in FP-unresponsive cases ( $n = 8$ ) as determined by microarray gene expression analysis (Figure 4a).<sup>9</sup> Furthermore, *LRRC31* mRNA expression decreased 18-fold ( $P < 0.05$ ) in diet-responsive cases ( $n = 10$ ), but did not change in diet-unresponsive cases ( $n = 5$ ) (Figure 4a). These data indicate that *LRRC31* mRNA is dynamically expressed as a function of disease activity.

### LRRC31 expression correlates with esophageal eosinophilia and IL13 expression

*LRRC31* mRNA expression showed a strong positive correlation (Pearson's  $r = 0.60$ ,  $P < 0.01$ ) with esophageal eosinophil levels (Figure 4b) and with esophageal *IL13* mRNA expression

(Pearson's  $r = 0.60$ ,  $P < 0.0001$ ) (Figure 4c).<sup>7,9</sup> Esophageal *LRRC31* mRNA expression also had a strong positive correlation with chemokine (C-C motif) ligand 26 (*CCL26*) mRNA expression (Pearson's  $r = 0.65$ ,  $P < 0.0001$ ), an eosinophil chemokine and IL-13-induced gene (Figure 4d).<sup>9,11</sup> In contrast, *LRRC31* mRNA expression had a weak positive correlation with the eosinophil prodifferentiation, activation, and survival cytokine *IL5* (Pearson's  $r = 0.27$ ,  $P < 0.05$ ) (Figure 4e).<sup>16</sup>

### IL-13 induces LRRC31 in epithelial cells

Induction of *LRRC31* mRNA expression in IL-4-treated human bronchial epithelial cells and in IL-13-treated human tracheal epithelial cells has been reported previously (Supplementary Figure 1a, b online).<sup>17,18</sup> As we identified the colon as the tissue where *LRRC31* mRNA is most abundantly expressed, we treated Caco2-bbe cells (colorectal adenocarcinoma cells, brush border expressing clone) with IL-13 and found that *LRRC31* mRNA expression increased 2.7-fold ( $P < 0.05$ ) and *CCL26* mRNA expression increased 62-fold ( $P < 0.05$ ) as determined by qPCR analysis (Supplementary Figure 1c). Similarly, in primary esophageal epithelial cells treated with IL-13, *LRRC31* mRNA expression increased 28-fold ( $P < 0.05$ ) and *CCL26* mRNA expression increased 56-fold ( $P < 0.001$ ) as determined by microarray gene expression analysis (Supplementary Figure 1d).<sup>9</sup> We used qPCR analysis to replicate this observation in primary esophageal epithelial cells derived from separate patients, treated with IL-13 (100 ng ml<sup>-1</sup>, 48 h), and found that *LRRC31* mRNA expression increased 4.8-fold ( $P < 0.01$ ) and *CCL26* mRNA expression increased 1,705-fold ( $P < 0.0001$ ) (Figure 5a). To determine if *LRRC31* was a direct target of IL-13-STAT6 (signal transducer and activator of transcription 6) signaling, we identified two putative STAT6 binding sites within the 2 kb upstream putative promoter of *LRRC31* using publicly available ChIP-Seq data from CD4<sup>+</sup> T cells (Supplementary Figure 2a).<sup>19</sup> However, using a luciferase reporter assay, we observed a 1.2-fold decrease in luciferase activity in TE-7 esophageal epithelial cells transfected with the *LRRC31* gene promoter following IL-13 treatment; as a

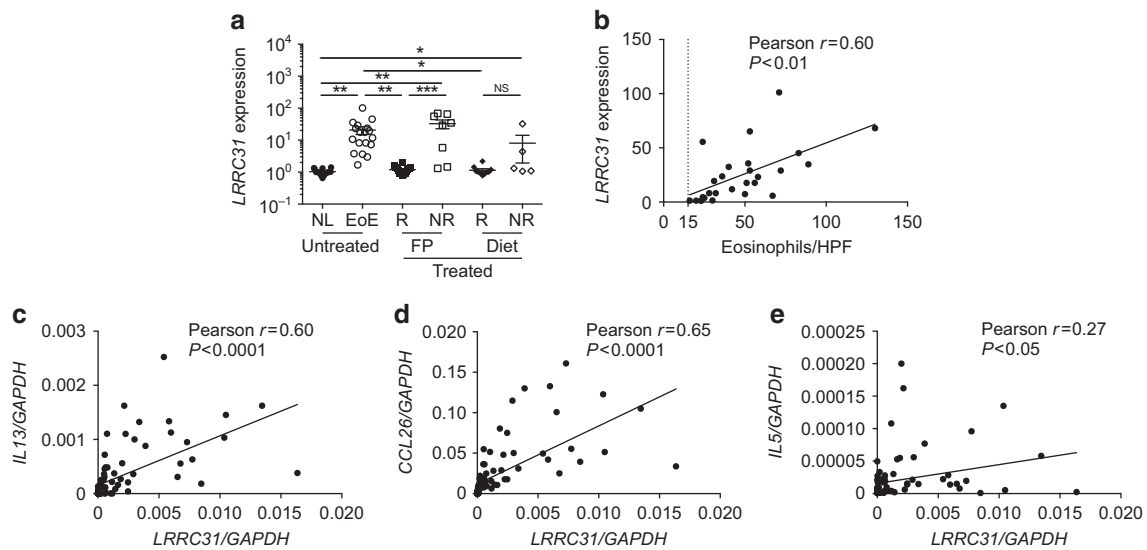


**Figure 4** Leucine-rich repeat-containing protein 31 (*LRRC31*) correlation with esophageal eosinophilia and disease-associated gene expression. (a) Normalized *LRRC31* mRNA expression in esophageal biopsies of patients with untreated, fluticasone propionate (FP)-treated, or diet therapy-treated eosinophilic esophagitis (EoE) (14 normal controls (NL), 18 active eosinophilic esophagitis (EoE), 24 EoE treatment responders (R), 12 EoE treatment nonresponders (NR)) by microarray gene expression analysis. (b) Correlation of biopsy eosinophil count per high-power field (hpf) and normalized *LRRC31* mRNA expression in esophageal biopsies of patients with active EoE as determined by microarray gene expression analysis. Dotted line represents 15 eosinophils per hpf, the diagnostic threshold for EoE. Correlation of normalized *LRRC31* mRNA expression with normalized (c) *IL13*, (d) *CCL26* (d), and (e) *IL5* mRNA expression in esophageal biopsies of patients with active EoE as determined by qPCR analysis. For (a), data points represent individual subjects and data are represented as the mean  $\pm$  s.e.m. \* $P < 0.05$ , \*\* $P < 0.01$ , and \*\*\* $P < 0.001$ . NS, not significant.

positive control, the *CCL26* 2 kb upstream gene promoter had an 11-fold increase in luciferase activity following IL-13 treatment (Supplementary Figure 2b). Interestingly, *LRRC31* mRNA expression was not induced in EPC2 esophageal epithelial cells grown *in vitro* in submerged, undifferentiated monolayer culture (data not shown).

Therefore, we used EPC2s grown at the ALI in high-calcium conditions to induce differentiation and stratification, to model the *in vivo* esophageal epithelium more accurately (Figure 5b). Briefly, EPC2s were grown on a permeable transwell support in low calcium ( $[Ca^{2+}] = 0.09$  mM) for 2 days, followed by high calcium ( $[Ca^{2+}] = 1.8$  mM) for the next 12 days. Cells were brought to the ALI on day 7 and grown until day 14 at the ALI, resulting in an *in vitro* stratified squamous epithelium. Hematoxylin and eosin (H&E)-stained differentiated EPC2s at day 14 demonstrated well-defined SC and SG (Figure 5c). The addition of IL-13 at day 8 to EPC2s grown at the ALI, followed by H&E staining at day 14 showed disrupted formation of the epithelium with loss of the SC and expansion of the SG, a characteristic seen in the esophagus of patients with active EoE (Figure 5c).<sup>1,7</sup> In addition, differentiated EPC2s, verified by increased *KRT10* mRNA expression, demonstrated a marked increase in barrier function, assessed by increased TER and decreased paracellular flux.<sup>7</sup> IL-13 treatment decreased *KRT10* mRNA expression levels 3.1-fold ( $P < 0.05$ ), impaired barrier formation as indicated by decreased TER (1.9-fold,  $P < 0.05$ ), and increased paracellular flux (2.8-fold,  $P < 0.05$ ), modeling the IBF observed in the esophageal epithelium of patients with active EoE (Figure 5d–f). Interestingly, *LRRC31* mRNA expression was

increased 312-fold ( $P < 0.01$ ) and *CCL26* mRNA expression increased 4,853-fold ( $P < 0.01$ ) in IL-13-treated, differentiated EPC2s compared with untreated, differentiated EPC2s, as demonstrated by qPCR analysis (Figure 5g). In addition, *LRRC31* protein expression was detectable by western blot analysis in IL-13-treated, differentiated EPC2s, and its expression relative to heat-shock protein 90 (HSP90) loading control was increased 14-fold ( $P < 0.05$ ) compared with untreated, differentiated EPC2s (Figure 5h). These data show that *LRRC31* mRNA and protein were induced in epithelial cells treated with IL-13.

#### Overexpression of *LRRC31* increases barrier function

To understand the function of *LRRC31* in the esophageal epithelium, we overexpressed *LRRC31* in differentiated EPC2s. Briefly, EPC2s were transduced with either empty vector (control) or FLAG epitope-tagged *LRRC31* lentiviral expression constructs and grown at the ALI. *LRRC31* mRNA expression increased 36-fold ( $P < 0.05$ ) in IL-13-treated control EPC2s and 4,423-fold ( $P < 0.05$ ) in untreated *LRRC31*-overexpressing EPC2s when compared with untreated control EPC2s as determined by qPCR analysis (Figure 6a). Following IL-13 treatment, *LRRC31* mRNA expression showed a 154-fold increase ( $P < 0.05$ ) in *LRRC31*-overexpressing EPC2s compared with IL-13-treated control EPC2s as determined by qPCR analysis (Figure 6a). *CCL26* mRNA expression increased 73-fold ( $P < 0.01$ ) in IL-13-treated control EPC2s and 148-fold ( $P < 0.01$ ) in IL-13-treated *LRRC31*-overexpressing EPC2s as determined by qPCR analysis (Figure 6a). *KRT10* mRNA expression decreased 3.2-fold ( $P < 0.05$ ) in IL-13-

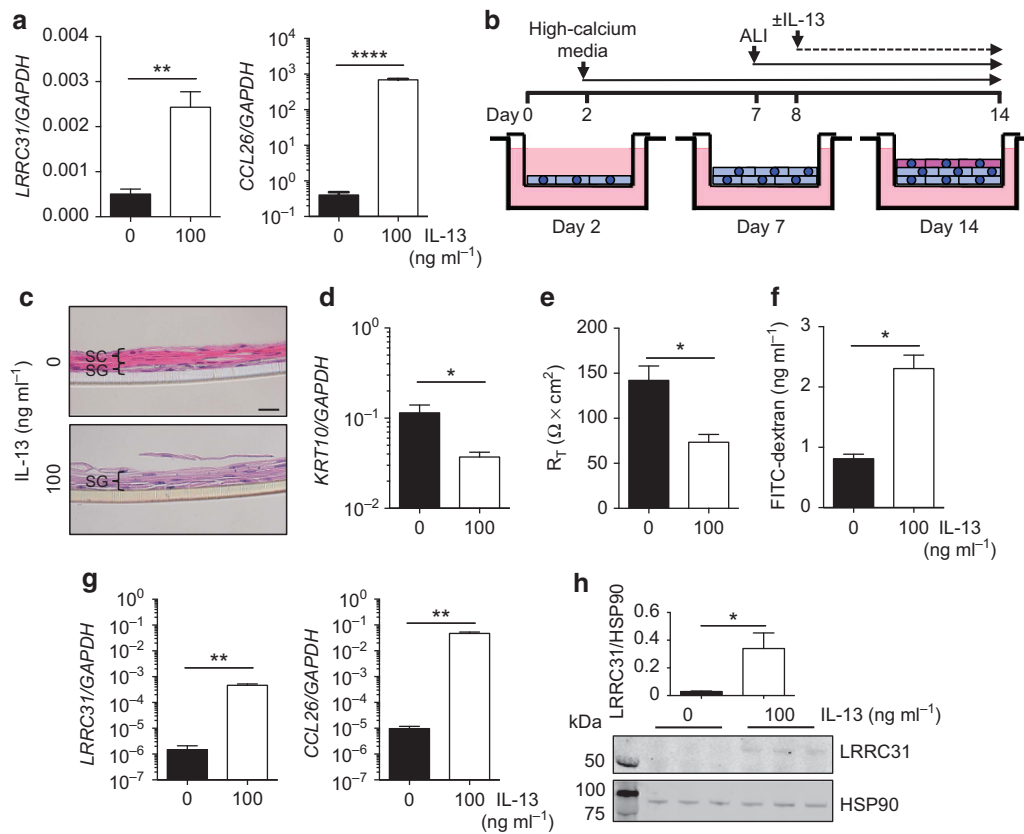


**Figure 5** Leucine-rich repeat-containing protein 31 (*LRRC31*) expression in esophageal epithelial cells. **(a)** Normalized *LRRC31* and *CCL26* mRNA expression in primary esophageal epithelial cells treated with interleukin-13 (IL-13) ( $100 \text{ ng ml}^{-1}$ ) for 48 h as determined by qPCR analysis. **(b)** Differentiated esophageal epithelial cells (EPC2) esophageal epithelial cells were grown for 12 days in high-calcium media. Cells were brought to the air-liquid interface (ALI) starting at day 7, and  $\pm$ IL-13 treatment ( $100 \text{ ng ml}^{-1}$ ) started at day 8. **(c)** Hematoxylin and eosin (H&E)-stained sections of differentiated EPC2s at day 14. Stratum corneum (SC, pink layer) and stratum germinativum (SG, purple layer) are indicated. A representative experiment is shown ( $n=3$ ). Bar =  $20 \mu\text{m}$ . **(d)** Normalized *KRT10* mRNA expression in differentiated EPC2s at day 14 as determined by qPCR. A representative experiment is shown ( $n=3$ ). RT, resistance. **(e)** Transepithelial electrical resistance (TER) measured across differentiated EPC2s at day 14. A representative experiment is shown ( $n=3$ ). **(f)** Fluorescein isothiocyanate (FITC)-dextran (3–5 kDa) paracellular flux measured at 3 h after FITC-dextran was added to luminal surface of differentiated EPC2s at day 14. A representative experiment is shown ( $n=3$ ). **(g)** Normalized *LRRC31* and *CCL26* mRNA expression in differentiated EPC2s at day 14 as determined by qPCR. A representative experiment is shown ( $n=3$ ). **(h)** *LRRC31* protein expression in differentiated EPC2s at day 14 as determined by western blot analysis. Image shown is a representative experiment ( $n=3$ ); heat-shock protein 90 (HSP90) (90 kDa) loading control is shown. Left lane is the molecular weight ladder. Expression level of *LRRC31* protein was quantified and normalized to the level of HSP90 protein. For **(a and d–h)**, data are represented as the mean  $\pm$  s.e.m.; \* $P < 0.05$ , \*\* $P < 0.01$ , and \*\*\*\* $P < 0.0001$ .

treated control EPC2s and 3.2-fold ( $P < 0.01$ ) in IL-13-treated *LRRC31*-overexpressing EPC2s compared with untreated EPC2s as determined by qPCR analysis (**Figure 6a**). Western blot analysis confirmed a marked increase in *LRRC31* protein expression in *LRRC31*-overexpressing EPC2s compared with control EPC2s (**Figure 6b**).

H&E staining of untreated control EPC2s and untreated *LRRC31*-overexpressing EPC2s showed similar histology (**Figure 6c**). Interestingly, IL-13-treated control EPC2s had increased epithelial thickness (1.8-fold,  $P < 0.05$ ) with loss of the SC and expansion of the SG when compared with untreated control EPC2s (**Figure 6d**). However, untreated and IL-13-treated *LRRC31*-overexpressing EPC2s had similar epithelial thickness and morphology (**Figures 6c, d**). In assessing the IBF of IL-13-treated EPC2s, we found TER decreased 2.2-fold ( $P < 0.001$ ) in control EPC2s and 2.0-fold ( $P < 0.01$ ) in *LRRC31*-overexpressing EPC2s (**Figure 6e**). However, untreated

*LRRC31*-overexpressing EPC2s had 1.9-fold increased ( $P < 0.05$ ) TER when compared with untreated control EPC2s, and IL-13-treated *LRRC31*-overexpressing EPC2s had 2.0-fold increased ( $P < 0.001$ ) TER when compared with IL-13-treated control EPC2s (**Figure 6e**). Similarly, IL-13 treatment increased paracellular flux 2.1-fold ( $P < 0.05$ ) in control EPC2s and 2.2-fold ( $P < 0.05$ ) in *LRRC31*-overexpressing EPC2s (**Figure 6f**). Furthermore, untreated *LRRC31*-overexpressing EPC2s had 2.8-fold increased ( $P < 0.05$ ) paracellular flux compared with untreated control EPC2s (**Figure 6f**). Taken together, these data suggest a function for *LRRC31* in regulating the esophageal epithelial barrier function *in vitro*.

### **LRRC31 regulates epithelial serine proteases**

We undertook RNA-sequencing analysis to gain insight into the mechanism by which *LRRC31* regulated the epithelial

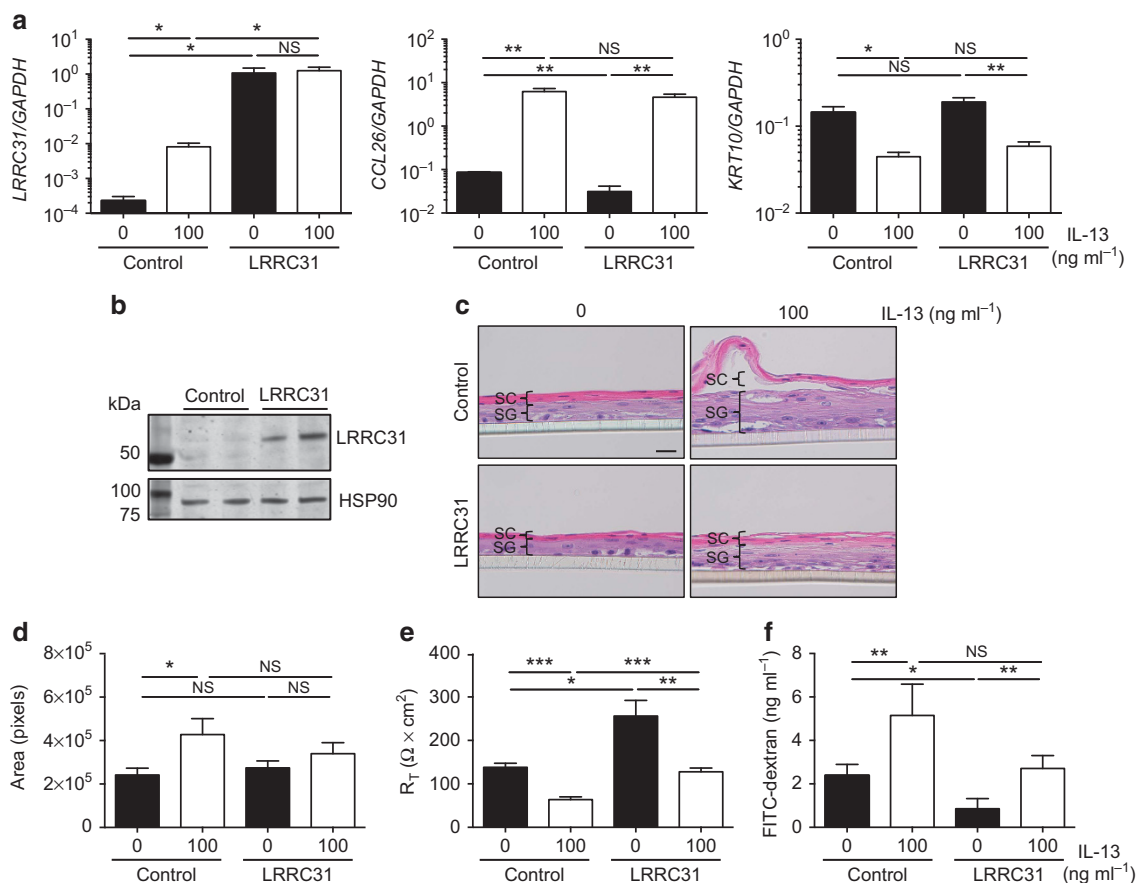


**Figure 6** Epithelial barrier function in differentiated leucine-rich repeat-containing protein 31 (LRR31)-overexpressing differentiated esophageal epithelial cells (EPC2) cells. EPC2 esophageal epithelial cells transduced with either empty vector (control) or flag-epitope-tagged LRR31 lentiviral expression constructs were cultured as described in **Figure 5b**. **(a)** Normalized *LRR31*, *CCL26* and *KRT10* mRNA expression in differentiated control and LRR31-overexpressing (LRR31) EPC2s at day 14 as determined by qPCR analysis. A representative experiment is shown ( $n=3$ ). **(b)** LRR31 (61.5 kDa) protein expression in differentiated control and LRR31-overexpressing EPC2s at day 14 as determined by western blot analysis. Image shown is a representative experiment ( $n=3$ ); heat-shock protein 90 (HSP90) (90 kDa) loading control is shown. Left lane is the molecular weight ladder. **(c)** Hematoxylin and eosin (H&E) staining of differentiated control and LRR31-overexpressing EPC2s at day 14. Bar = 20  $\mu\text{m}$ . A representative experiment is shown ( $n=3$ ). **(d)** Cross-sectional area of H&E-stained sections from differentiated control and LRR31-overexpressing EPC2s at day 14. A representative experiment is shown ( $n=3$ ). **(e)** TER measured across differentiated control and LRR31-overexpressing EPC2s at day 14. A representative experiment is shown ( $n=3$ ). RT, resistance. **(f)** FITC-dextran (3–5 kDa) paracellular flux measured at 3 h after FITC-dextran was added to luminal surface of differentiated control and LRR31-overexpressing EPC2s at day 14. A representative experiment is shown ( $n=3$ ). For **(a)** and **(d–f)**, data are represented as the mean  $\pm$  s.e.m. \* $P<0.05$ , \*\* $P<0.01$ , and \*\*\* $P<0.001$ . NS, not significant.

barrier. Applying a moderated  $t$ -test with Benjamini–Hochberg false discovery rate analysis ( $P<0.05$ ), we identified 38 genes that changed  $\geq 1.5$ -fold in differentiated LRR31-overexpressing EPC2s when compared with control EPC2s (**Figure 7a**). As expected, the most highly upregulated mRNA transcript in the LRR31-overexpressing EPC2s was *LRR31*. Among the downregulated mRNA transcripts was *noggin* (*NOG*), a ligand that antagonizes bone morphogenetic proteins (BMPs), which are members of the transforming growth factor- $\beta$  family of cytokines.<sup>20</sup> Interestingly, gene ontology analysis carried out using the Database for Annotation, Visualization, and Integrated Discovery (DAVID) identified one cluster of five KLK serine proteases, *KLK5*, *KLK7*, *KLK11*, *KLK12*, and *KLK13*, with an enrichment score of 2.71, which were downregulated in LRR31-overexpressing EPC2s, suggesting that LRR31 may be a negative regulator of KLK proteases.<sup>21,22</sup>

We further showed decreased *KLK5* (4.74-fold,  $P<0.01$ ), *KLK7* (1.68-fold,  $P<0.05$ ), *KLK11* (1.35-fold,  $P<0.05$ ), and *KLK13* (1.81-fold,  $P<0.01$ ) mRNA expression in LRR31-overexpressing EPC2s in an independent experiment by qPCR analysis; *KLK1* mRNA expression was unchanged as a control (**Figure 7b**). Moreover, using a protease array, we detected decreased protein expression of *KLK5* (1.15-fold,  $P<0.05$ ), *KLK7* (2.7-fold,  $P<0.05$ ), *KLK11* (1.4-fold,  $P<0.01$ ), and *KLK13* (2.1-fold,  $P<0.05$ ) in the supernatants of LRR31-overexpressing EPC2s; *KLK10* protein expression was unchanged as a control (**Figure 7c**). The supernatants from LRR31-overexpressing EPC2s also had decreased KLK protease activity (1.25-fold,  $P<0.05$ ), assessed using a fluorogenic peptide substrate specific for *KLK4*, *KLK5*, *KLK8*, *KLK13*, and *KLK14* (**Figure 7d**). Taken together, these data support the observation that KLK proteases are negatively regulated by LRR31.

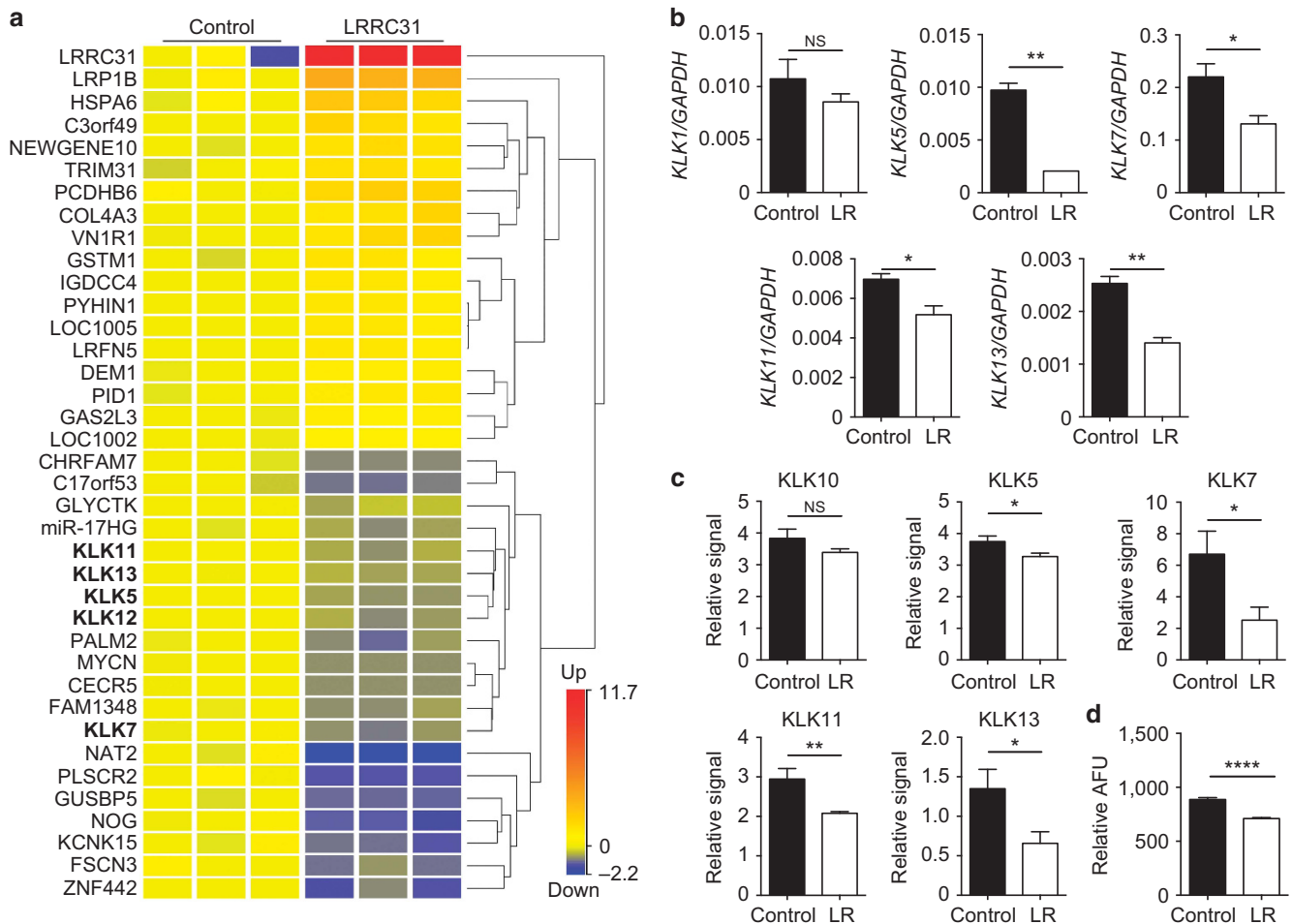


**Figure 7** Differentiated leucine-rich repeat-containing protein 31 (LRRC31)-overexpressing differentiated esophageal epithelial cell (EPC2) transcriptome. **(a)** Heat diagram representing RNA sequencing analysis of differentiated empty vector (control) and LRRC31-overexpressing EPC2s. Differentially expressed genes were identified by filtering on fragments per kilobase per million (FPKM)  $\geq 1$ , moderated *t*-test with Benjamini–Hochberg false discovery rate ( $P < 0.05$ ), and fold change  $\geq 1.5$ . Kallikrein (KLK) family members are bolded. **(b)** Normalized *KLK1*, *KLK5*, *KLK7*, *KLK11*, and *KLK13* mRNA expression in differentiated control and LRRC31-overexpressing (LR) EPC2s as determined by qPCR analysis. A representative experiment is shown ( $n = 3$ ). **(c)** KLK10, KLK5, KLK7, KLK11, and KLK13 protein expression normalized to total protein in differentiated control and LRRC31-overexpressing EPC2 supernatants as determined by protease array analysis. A representative experiment is shown ( $n = 3$ ). **(d)** KLK serine protease activity in differentiated control and LRRC31-overexpressing EPC2 supernatants (AFU, arbitrary fluorescence units normalized to total protein). A representative experiment is shown ( $n = 3$ ). For **(b–d)**, data are represented as the mean  $\pm$  s.e.m. \* $P < 0.05$ , \*\* $P < 0.01$ , and \*\*\*\* $P < 0.0001$ . NS, not significant.

### Loss of LRRC31 increases KLK expression

To understand the function of LRRC31 in response to IL-13 treatment, we used short-hairpin RNA (shRNA) to silence *LRRC31* mRNA expression in differentiated EPC2s. Briefly, EPC2s were transduced with non-silencing control (NSC) or LRRC31-specific shRNA-containing lentiviral expression constructs and grown at the ALI. At baseline, the *LRRC31* mRNA expression was below the limit of detection by qPCR ( $\geq 34 C_T$ ). Following IL-13 treatment, *LRRC31* mRNA expression was detected in NSC EPC2s and was reduced 31-fold ( $P < 0.01$ ) in *LRRC31* gene-silenced EPC2s (**Figure 8a,b**). As a control, *CCL26* and *KRT10* mRNA expression was not decreased in *LRRC31* gene-silenced EPC2s (**Figure 8a**). Notably, following IL-13 treatment *LRRC31* gene-silenced EPC2s had suprabasal detachment within the SG (**Figure 8c** and **Supplementary Figure 3**).

As LRRC31-overexpressing EPC2s had decreased expression of KLK proteases, we used qPCR analysis to determine the expression of KLK mRNA in IL-13-treated *LRRC31* gene-silenced EPC2s. We identified increased mRNA expression levels for *KLK7* (2.4-fold,  $P < 0.05$ ), *KLK11* (3.9-fold,  $P < 0.01$ ), and *KLK13* (9.5-fold,  $P < 0.05$ ) in IL-13-treated *LRRC31* gene-silenced EPC2s compared with NSC EPC2s (**Figure 8d**). However, *KLK1* and *KLK5* mRNA expression did not change in IL-13-treated *LRRC31* gene-silenced EPC2s compared with NSC EPC2s (**Figure 8d**).

In addition, TER decreased 1.4-fold ( $P < 0.01$ ) in IL-13-treated NSC EPC2s, but was similar in untreated and IL-13-treated *LRRC31* gene-silenced EPC2s (**Figure 8e**). However, the TER in untreated *LRRC31* gene-silenced EPC2s was increased 1.5-fold ( $P < 0.05$ ) compared with untreated NSC EPC2s, and the TER in IL-13-treated *LRRC31* gene-silenced

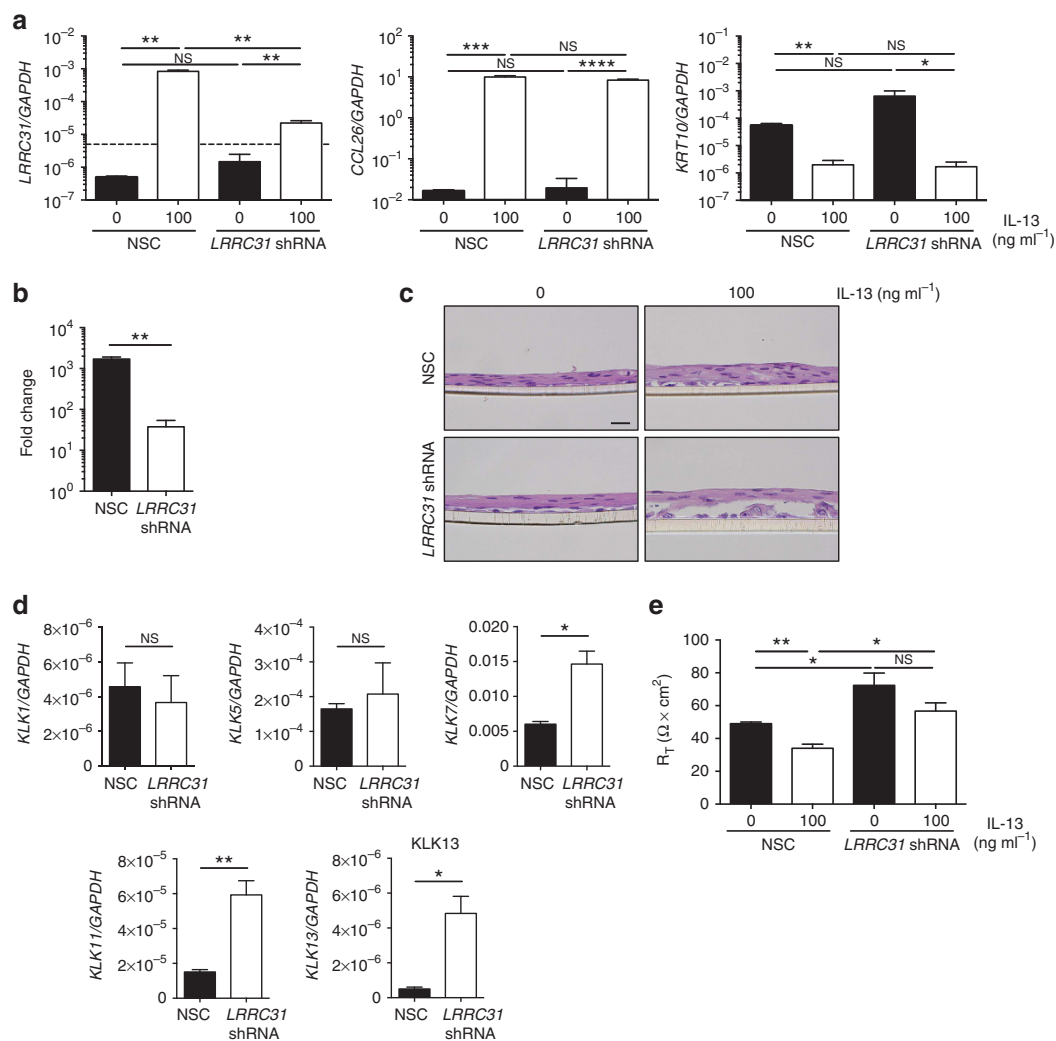


**Figure 8** Kallikrein (KLK) expression following leucine-rich repeat-containing protein 31 (*LRRC31*) gene-silencing in differentiated EPC2 cells. EPC2 esophageal epithelial cells transduced with either non-silencing control (NSC) or *LRRC31* short hairpin RNA (*LRRC31* shRNA) lentiviral expression constructs were cultured as described in **Figure 5b**. **(a)** Normalized *LRRC31* and *CCL26* mRNA expression in differentiated NSC and *LRRC31* shRNA EPC2s at day 14 as determined by qPCR analysis. Dashed line represents limit of detection. **(b)** Fold change in *LRRC31* mRNA expression following IL-13 treatment in differentiated NSC and *LRRC31* shRNA EPC2s at day 14. **(c)** Hematoxylin and eosin (H&E)-stained sections from differentiated NSC and *LRRC31* shRNA EPC2s at day 14. **(d)** Normalized *KLK1*, *KLK5*, *KLK7*, *KLK11*, and *KLK13* mRNA expression in IL-13-treated differentiated NSC and *LRRC31* shRNA EPC2 cells at day 14 as determined by qPCR. **(e)** Transepithelial electrical resistance (TER) measured across differentiated NSC and *LRRC31* shRNA EPC2s at day 14. RT, resistance. For **(a–e)**, a representative experiment is shown ( $n=3$ ). For **(a, b, d, e)**, data are represented as the mean  $\pm$  s.e.m. \* $P<0.05$ , \*\* $P<0.01$ , \*\*\* $P<0.001$ , and \*\*\*\* $P<0.0001$ . NS, not significant.

EPC2s was increased 1.7-fold ( $P<0.05$ ) compared with IL-13-treated NSC EPC2s (**Figure 8e**). These data show that IL-13-treated, differentiated *LRRC31* gene-silenced EPC2s have disrupted epithelial morphology and decreased IBF, which may result from increased KLK expression.

#### KLK expression in EoE and in response to IL-13

We sought to characterize the changes in KLK expression in the esophagus of patients with active EoE and in primary esophageal epithelial cells following IL-13 treatment. In the esophagus, we identified downregulation of *KLK8* ( $P<0.05$ ) and *KLK13* ( $P<0.05$ ) mRNA expression specifically in patients with active EoE compared with control patients, using analysis

of variance ( $P<0.05$ ) on microarray gene expression data (**Figure 9a**). In contrast, there was increased *KLK7* ( $P<0.05$ ) and *KLK10* ( $P<0.01$ ) mRNA expression in both chronic esophagitis and EoE. In primary esophageal epithelial cells treated with IL-13, we identified downregulation of *KLK5* ( $P<0.05$ ), *KLK8* ( $P<0.05$ ), and *KLK10* ( $P<0.05$ ) mRNA expression using a moderated *t*-test analysis ( $P<0.05$ ) (**Figure 9b**). No KLKs were significantly upregulated by IL-13 treatment of primary esophageal epithelial cells. Taken together, these data show dysregulation of KLKs, specifically downregulation of *KLK13* and *KLK5* in EoE and in primary esophageal epithelial cells following IL-13 treatment, respectively.



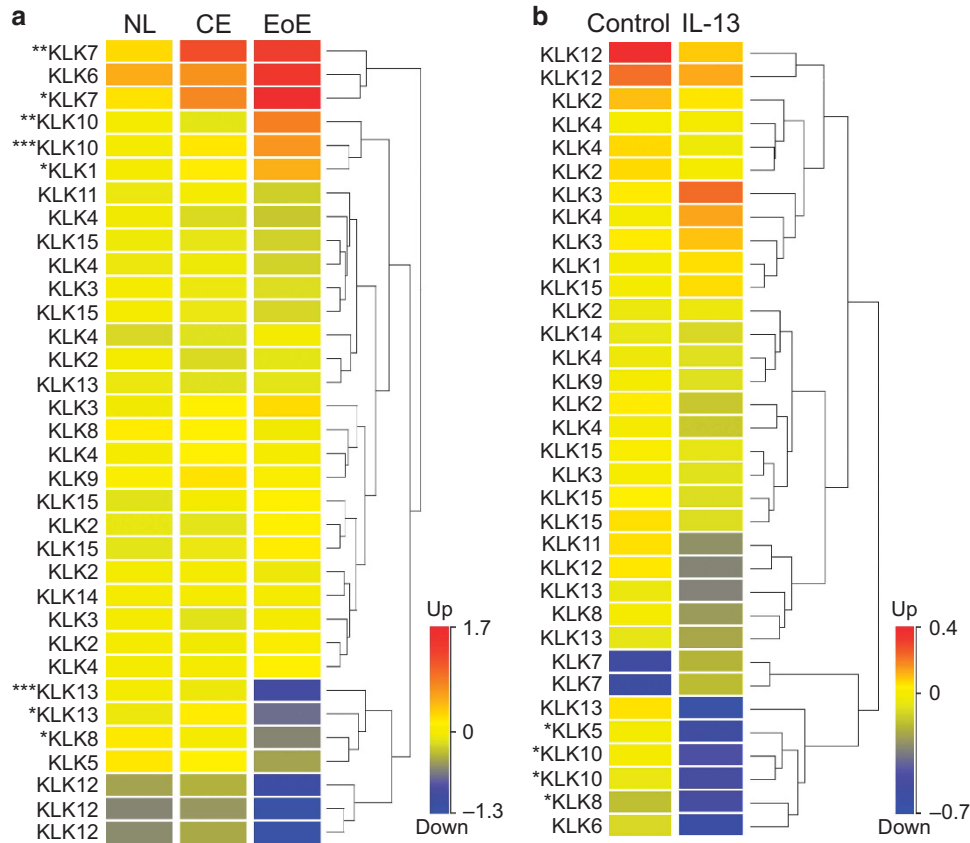


**Figure 9** Kallikrein (KLK) expression in esophageal biopsies and interleukin-13 (IL-13)-treated primary esophageal epithelial cells. **(a)** Heat diagram of KLK mRNA expression in esophageal biopsies of NL, chronic esophagitis (CE), and eosinophilic esophagitis (EoE) patients as determined by microarray gene expression analysis. **(b)** Heat diagram of KLK mRNA expression in primary esophageal epithelial cells stimulated with IL-13 (100 ng ml<sup>-1</sup>) for 48 h determined by microarray gene expression analysis. Each row represents one microarray probe. Hierarchical clustering used to analyze data and generate heat diagrams. Statistical analysis by **(a)** analysis of variance (ANOVA) and **(b)** moderated *t*-test with *P*<0.05. \**P*<0.05, \*\**P*<0.01, and \*\*\**P*<0.001.

**DISCUSSION**

The data presented herein characterize the expression, cytokine regulation, and role of *LRRC31* in esophageal cells. We identified *LRRC31* as a dysregulated gene in both the active EoE esophagus and in esophageal epithelial cells treated with IL-13. We provide evidence that *LRRC31* mRNA and protein is increased in the esophagus of patients with EoE, is normalized following FP and diet therapy, but remains increased in patients who had EoE resistant to therapy. It is notable that even diet non-responders had a decrease in *LRRC31* mRNA expression, suggesting that its change may be an early biomarker of response. *LRRC31* mRNA expression significantly correlated with biopsy eosinophils, *IL13*, and *CCL26* mRNA expression and was induced by IL-13 in differentiated esophageal epithelial cells. Furthermore, *LRRC31*-overexpressing EPC2s had increased epithelial barrier function in parallel with decreased KLK protein expression and protease activity. Several KLKs expressed in the esophagus were dysregulated in EoE and in epithelial cells following IL-13 treatment, which overlapped with KLKs dysregulated in differentiated *LRRC31*-overexpressing EPC2s. Taken together, we propose that *LRRC31* is induced in the esophageal epithelium by IL-13 and regulates esophageal epithelial barrier function likely by

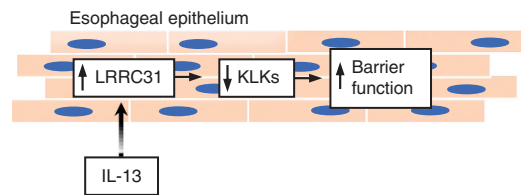


**Figure 10** Function of leucine-rich repeat-containing protein 31 (*LRRC31*) in the esophageal epithelium. Interleukin-13 (IL-13) induces *LRRC31* expression in esophageal epithelial cells, decreasing the expression of specific KLKs and increasing barrier function.

modulating expression and activity of KLKs, at least in part (**Figure 10**).

To understand how *LRRC31* may regulate esophageal epithelial barrier function, we undertook RNA sequencing analysis of differentiated *LRRC31*-overexpressing EPC2s. Interestingly, overexpressing *LRRC31* resulted in the down-regulation of *NOG* mRNA expression. *NOG* is an antagonist of the BMP signaling pathway, which regulates esophageal differentiation during development.<sup>20,23</sup> Interestingly, BMP signaling was shown to be active in differentiated squamous epithelium but not in basal progenitor cells, which express

follistatin, another BMP antagonist similar to NOG.<sup>20</sup> In both human esophageal biopsies from EoE patients and in a mouse model of EoE, reduced esophageal epithelial squamous differentiation is associated with high levels of follistatin and disrupted BMP signaling.<sup>20</sup> Thus, downregulation of NOG in LRRC31-overexpressing EPC2s supports a role for LRRC31 as a negative regulator of esophageal epithelial differentiation, possibly contributing to IBF.

Five KLK serine proteases, which have been shown to regulate skin barrier function in atopic dermatitis, were also downregulated in differentiated LRRC31-overexpressing EPC2s.<sup>12</sup> This finding was particularly notable considering the recent association of genetic variants in the intracellular cysteine protease calpain-14 (CAPN14) in patients with EoE, and emerging literature indicating that KLKs and CAPNs share common substrates, for example, KLK6 and CAPN1 both cleave  $\alpha$ -synuclein in neurons.<sup>5,12,24</sup> KLKs are extracellular proteases that are secreted in the SC of stratified squamous epithelium and cleave substrates such as DSG1, corneodesmosin, and desmocollins.<sup>12</sup> Interestingly, DSG1 is downregulated in the esophagus in EoE and in primary esophageal epithelial cells following IL-13 treatment, and gene silencing of DSG1 in differentiated EPC2s resulted in IBF *in vitro*.<sup>7</sup> It is interesting to speculate that the balance between esophageal epithelial proteases such as CAPNs and KLKs, and protease inhibitors such as Kazal-type serine protease inhibitors and serine protease inhibitors, may be lost, subsequently compromising the epithelial barrier function, as occurs in atopic dermatitis.<sup>12</sup> *In vitro* models may not accurately replicate the balance between proteases or the complex biological state found *in vivo*. For example, the barrier function in LRRC31-overexpressing EPC2 cells may have increased in the absence of IL-13, and upon IL-13 treatment decreased similar to control EPC2 cells, because additional molecules in the LRRC31 pathway were not expressed in the absence of IL-13 treatment in EPC2 cells. Alternatively, LRRC31 may be counterregulatory, a function that is further supported by gene silencing of LRRC31 in differentiated EPC2s.

Gene silencing of LRRC31 in differentiated EPC2s showed suprabasal detachment of the epithelium when treated with IL-13. It is notable that LRRC31 gene-silenced EPC2s had modulated barrier function using TER but not paracellular flux (Supplementary Figure 4). LRRC31 gene-silenced EPC2s also had increased mRNA expression of KLK7, KLK11, and KLK13 following IL-13 treatment. These data further support a role for LRRC31 in regulating KLK expression, activity, and protease equilibrium, which subsequently disrupts normal differentiation of non-keratinized stratified squamous epithelium *in vitro*. Interestingly, KLKs are dysregulated in EoE and in IL-13-treated primary esophageal epithelial cells in a manner that overlaps with LRRC31-overexpressing EPC2s. Thus, IL-13-induced LRRC31 may be specifically regulating a subset of KLKs in the esophageal epithelial response to IL-13 and in EoE.

On the basis of its primary amino-acid sequence, the primary isoform of LRRC31 (Q6UY01-1; 552 amino acids) is predicted to contain nine LRRs (Supplementary Figure 5a).

Additionally, LRRC31 contains a putative nuclear export signal (amino acids 113–121) and a nuclear localization signal (amino acids 517–545).<sup>25–27</sup> Differential exon splicing of LRRC31 produces two additional translated isoforms (Q6UY01-2 and Q6UY01-3 are 496 and 346 amino acids, respectively) that each possess a different complement of LRRs compared with the primary isoform (Supplementary Figure 5a). Using the I-TASSER (Iterative Threading Assembly Refinement) server for protein and structural predictions, LRRC31 is predicted to have a horseshoe-shaped tertiary structure with a hydrophobic substrate-binding pocket (Supplementary Figure 5b).<sup>28</sup> This structure suggests that LRRC31 participates in protein–protein interactions. Ribonuclease/angiogenin inhibitor 1, a ribonuclease inhibitor that binds to endogenous and exogenous ribonucleases to block ribonuclease activity, shared the highest homology score with LRRC31 (score = 224; *E*-value =  $1 \times 10^{-19}$ ) (Supplementary Figure 6a).<sup>29,30</sup> Additional homologous molecules include other members of the LRR-containing family of proteins such as LRRC32 and LRRC34, members of the NLRP (NACHT (NAIP—neuronal apoptosis inhibitor protein, CIITA—class II major histocompatibility complex transactivator, HET-E—incompatibility locus protein from *Podospora anserine*, TP1—telomerase-associated protein), LRR, and pyrin domain or nonobese diabetic-like receptor family pyrin domain containing) family of inflammasome proteins, antigen-sensing and immune-activating toll-like receptors, and adaptor proteins involved in ubiquitination and post-translational regulation of signaling pathways, such as flightless-1 homolog. These molecules participate in immunomodulatory events within cells.<sup>31–33</sup> It is notable that LRRC31 is highly conserved in humans, primates, and even through *Xenopus tropicalis*, consistent with a nonredundant function for this protein (Supplementary Figure 6b).<sup>34</sup>

In summary, we have shown that LRRC31 is specifically increased in EoE and dynamically expressed as a function of disease activity and therapy, and its expression is proportional to esophageal eosinophilia and IL13 mRNA expression. LRRC31 is induced by IL-13 treatment in epithelial cells, including differentiated esophageal epithelial cells. Considering the downregulation of KLKs and reduced KLK protease activity in differentiated LRRC31-overexpressing cells, we propose that LRRC31 is induced by IL-13 and regulates epithelial barrier function in the esophagus, possibly by modulating the expression of tissue KLKs.

## METHODS

**Patient sample selection.** Diagnosis was established based on the maximum eosinophil count of >15 per  $\times 400$  high-power field (hpf).<sup>11</sup> Normal control (NL) patients were defined as having no history of EoE, 0 eosinophils per hpf in the esophagus at the time of biopsy, and no concomitant swallowed glucocorticoid treatment. EoE patients were defined as having >15 eosinophils per hpf in the esophagus and no concomitant swallowed glucocorticoid treatment in patients on proton pump inhibitor therapy, except for the samples in the microarray experiment.<sup>11</sup> EoE patients receiving topical/swallowed FP glucocorticoid therapy and diet therapy were defined as

responders if they had  $\leq 1$  eosinophil per hpf at the time of biopsy or as nonresponders if they had  $\geq 6$  eosinophils per hpf.

**Microarray gene expression analysis.** For each patient, one distal esophageal biopsy sample was immersed in RNAlater (Qiagen, Hilden, Germany) and total RNA was extracted using the RNeasy Mini Kit (Qiagen). Hybridization to human Affymetrix U133 Plus 2.0 GeneChip DNA microarray (Affymetrix, Santa Clara, CA) was performed by the Microarray Core at Cincinnati Children's Hospital Medical Center (CCHMC).<sup>35</sup> Gene transcript levels were determined following quantification and normalization of microarray data using GeneSpring (Agilent Technologies, Santa Clara, CA).

**RNA sequencing analysis.** RNA isolated from esophageal biopsies or differentiated EPC2s was subjected to RNA sequencing at the Gene Discovery and Genetic Variation Core at CCHMC.<sup>7</sup> The paired-end sequencing reads were aligned against the GRCh37 genome model using TopHat 2.04 with Bowtie 2.03.<sup>36,37</sup> The separate alignments were then merged using Cuffmerge with RefSeq gene models as a reference. The aligned reads were quantified for differential expression analysis using Cuffdiff.<sup>38</sup> Normalization and statistical analysis was performed using GeneSpring (Agilent Technologies).

**qPCR analysis.** Total RNA (500 ng) was DNAase treated, and complementary DNA was generated using the iScript Complementary DNA Synthesis Kit (Bio-Rad Laboratories, Hercules, CA). qPCR was performed with the Applied Biosystems Incorporated 7900HT Fast Real-Time System (Life Technologies, Grand Island, NY) and LightCycler FastStart DNA Master SYBR Green as a ready-to-use reaction mix with ROX (Roche, Basel, Switzerland). Relative expression was calculated using a standard curve method, as described.<sup>39,40</sup> Results were normalized to *GAPDH* (glyceraldehyde 3-phosphate dehydrogenase) and fold induction compared with controls. cDNAs were amplified using TaqMan Gene Expression Assay (Hs00226845\_m1) and primers (Integrated DNA Technologies, Coralville, IA) (**Supplementary Table 1**).<sup>41</sup>

**Western blot analysis.** Total cell lysates were prepared from biopsy protein following Qiazol (Qiagen) RNA extraction. Briefly, protein pellets were resuspended in Laemmli buffer, incubated at 37 °C for 30 min, vortexed briefly, and heated to 95 °C for 5 min before electrophoresis. Cells were lysed using MPER lysis buffer (Sigma-Aldrich, St Louis, MO) supplemented with protease inhibitors (Roche) and sodium orthovanadate (10 mM) (Sigma-Aldrich). Loading buffer (Life Technologies) was added and samples were heated to 95 °C for 5 min, subjected to electrophoresis on 4–12% NuPAGE Bis-Tris gels (Life Technologies), transferred to nitrocellulose membranes (Life Technologies), and visualized using the Odyssey CLx system (LI-COR Biosciences, Lincoln, NE) with IRDye 800RD goat anti-rabbit (LI-COR) and IRDye 680RD goat anti-mouse (LI-COR Biosciences) secondary antibodies. Primary antibodies were: anti-LRRC31 (ab100379; Abcam PLC, Cambridge, UK) and anti-HSP90 (AF7247; R&D Systems, Minneapolis, MN). Blots were quantified using the Image Studio software (LI-COR).

**Primary cell culture.** Distal esophageal biopsy specimens from patients with EoE were collected and subsequently digested with trypsin, cultured in modified F-media (3:1F-12/Dulbecco's modified Eagle's medium) supplemented with fetal bovine serum (5%), adenine (24.2 mg ml<sup>-1</sup>), cholera toxin (1,024 nM), insulin (5 mg ml<sup>-1</sup>), hydrocortisone (0.4 mg ml<sup>-1</sup>), and epidermal growth factor (10 ng ml<sup>-1</sup>) in the presence of penicillin, streptomycin, and amphotericin (Life Technologies).<sup>9</sup> Cells were cultured for 2 weeks, and fibroblasts were depleted by means of differential trypsinization.

**EPC2 cell culture.** The esophageal epithelial cell line (human telomerase reverse transcriptase-immortalized EPC2 cell line) was a kind gift from Dr Anil Rustgi (University of Pennsylvania, Philadelphia,

PA).<sup>42–44</sup> EPC2s were cultured in keratinocyte serum-free media (Life Technologies) supplemented with bovine pituitary extract, epidermal growth factor, and amphotericin (Life Technologies). For differentiated EPC2 cell cultures, EPC2s were grown to confluence for 2 days while being fully submerged in low-calcium ([Ca<sup>2+</sup>] = 0.09 mM)-supplemented keratinocyte serum-free media on 0.4 μm pore-size permeable supports (Corning, Corning, NY). Confluent monolayers were then switched to high-calcium ([Ca<sup>2+</sup>] = 1.8 mM) media for an additional 5 days. The culture medium was removed from the inner chamber of the permeable support to expose the cell monolayer to the air interface at day 7. Differentiated EPC2s were analyzed 7 days after ALI induction.

**Lentiviral transduction.** EPC2s were transduced with virus containing FLAG epitope-tagged LRRC31 coding sequence or empty vector control using the pMIRNA1 lentiviral system (System-Biosciences, Mountain View, CA). EPC2s were transduced with shRNA targeting the coding sequence of *LRRC31* or an NSC shRNA using the GIPZ lentiviral system (Thermo Fisher Scientific, Waltham, MA). Lentiviral particles were prepared at the CCHMC Viral Vector Core. Twenty-four hours after transduction, EPC2s were selected for stable integration using puromycin (1 μg ml<sup>-1</sup>) for 48 h. Transduction efficiency was assessed by green fluorescent protein fluorescence and overexpression or silencing efficiency was assessed by qPCR compared with empty vector control-transduced cells.

**TER and paracellular flux assays.** For differentiated EPC2s, TER and 3–5 kDa FITC-dextran (Sigma-Aldrich) paracellular flux were measured at day 7 after ALI induction as previously described using an EVOM (World Precision Instruments, Sarasota, FL) and a fluorescence plate reader (BioTek, Winooski, VT), respectively.<sup>45</sup>

**Protease array and KLK activity assay.** Supernatants from differentiated EPC2s were collected and total protein was quantified using the BCA assay (Life Technologies). The Proteome Profiler Human Protease Array Kit (R&D Systems) was used to quantify protease expression, which was quantified using the Image Studio Software (LI-COR) and normalized to total protein. For the KLK activity assay, equal protein (1 μg) was mixed with Boc-V-P-R-AMC Fluorogenic Peptide Substrate (R&D Systems) and reaction buffer, and the plate containing the reactions was incubated overnight at 37 °C. The plate was read with excitation at 380 nm and emission at 460 nm using a fluorescence plate reader (BioTek).

**Luciferase activity assay.** The 2 kb upstream gene promoter for *LRRC31* was cloned into the pGL3-basic construct and co-transfected with pRL-TK into TE-7 cells, which were treated with IL-13 (100 ng ml<sup>-1</sup>) for 48 h. Luciferase activity was determined using the Dual-Luciferase Reporter Assay System (Promega, Madison, WI) as per the manufacturer instructions.

**Histological analyses.** Cross-sectional area of H&E-stained sections was calculated using thresholding image processing with ImageJ (US National Institutes of Health, Bethesda, MD).

**Statistical analyses.** Statistical significance was determined using a *t*-test and analysis of variance test. Pearson's correlation was used to test for correlated gene expression. All statistical analyses were performed using GraphPad Prism (GraphPad Software, La Jolla, CA).

**Study approvals.** For human subjects, written informed consent was obtained before a patient's enrollment in the studies, and all human studies were approved by the CCHMC Institutional Review Board (IRB protocol 2008-0090). All experiments involving mice were approved by the CCHMC IACUC.

**SUPPLEMENTARY MATERIAL** is linked to the online version of the paper at <http://www.nature.com/mi>

## ACKNOWLEDGMENTS

This work was supported in part by NIH U19 AI070235, NIH R01 DK076893, the PHS Grant P30 DK0789392 (CCHMC DNA Sequencing and Genotyping Facility, CCHMC Pathology Research Core, and CCHMC Viral Vector Core), the Food Allergy Research and Education, the Buckeye Foundation, and the Campaign Urging Research for Eosinophilic Diseases (CURED) Foundation. We thank Dr Rustgi (University of Pennsylvania) for the human telomerase reverse transcriptase-immortalized EPC2 cell line. We also thank Shawna Hottinger for editorial assistance, all of the participating families and the Cincinnati Center for Eosinophilic Disorders, and members of the Division of Allergy and Immunology.

## AUTHOR CONTRIBUTIONS

R.J.D., N.P.A., S.P.H., and M.E.R. were involved in study concept and design. R.J.D., J.M.C., T.W., and J.D.S. were involved in data acquisition. R.J.D. and M.E.R. analyzed and interpreted data. R.J.D., J.M.C., S.P.H., and M.E.R. were involved in the writing and critical revision of the manuscript.

## DISCLOSURE

M.E.R. has an equity interest in reslizumab (Teva Pharmaceuticals); is a consultant and has an equity interest in Receptos, Celsius Therapeutics, NKT Therapeutics, and Immune Pharmaceuticals; and is the inventor of several EoE-related patents owned by Cincinnati Children's Hospital Medical Center. S.P.H. is a consultant for Immune Pharmaceuticals. T.W. is the inventor of several EoE-related patents owned by Cincinnati Children's Hospital Medical Center. The other authors declared no conflict of interest.

© 2016 Society for Mucosal Immunology

## REFERENCES

- Liacouras, C.A. *et al.* Eosinophilic esophagitis: updated consensus recommendations for children and adults. *J. Allergy Clin. Immunol.* **128**, 3–20 (2011).
- Rothenberg, M.E. *et al.* Common variants at 5q22 associate with pediatric eosinophilic esophagitis. *Nat. Genet.* **42**, 289–291 (2010).
- Blanchard, C. *et al.* Coordinate interaction between IL-13 and epithelial differentiation cluster genes in eosinophilic esophagitis. *J. Immunol.* **184**, 4033–4041 (2010).
- Sherrill, J.D. & Rothenberg, M.E. Genetic dissection of eosinophilic esophagitis provides insight into disease pathogenesis and treatment strategies. *J. Allergy Clin. Immunol.* **128**, 23–32 (2011).
- Kottyan, L.C. *et al.* Genome-wide association analysis of eosinophilic esophagitis provides insight into the tissue specificity of this allergic disease. *Nat. Genet.* **46**, 895–900 (2014).
- Orlando, R.C. The integrity of the esophageal mucosa. Balance between offensive and defensive mechanisms. *Best. Pract. Res. Clin. Gastroenterol.* **24**, 873–882 (2010).
- Sherrill, J.D. *et al.* Desmoglein-1 regulates esophageal epithelial barrier function and immune responses in eosinophilic esophagitis. *Mucosal Immunol.* **7**, 718–729 (2014).
- Straumann, A., Bauer, M., Fischer, B., Blaser, K. & Simon, H.U. Idiopathic eosinophilic esophagitis is associated with a T(H)2-type allergic inflammatory response. *J. Allergy Clin. Immunol.* **108**, 954–961 (2001).
- Blanchard, C. *et al.* IL-13 involvement in eosinophilic esophagitis: transcriptome analysis and reversibility with glucocorticoids. *J. Allergy Clin. Immunol.* **120**, 1292–1300 (2007).
- Sherrill, J.D. *et al.* Analysis and expansion of the eosinophilic esophagitis transcriptome by RNA sequencing. *Genes Immun.* **15**, 361–369 (2014).
- Blanchard, C. *et al.* Eotaxin-3 and a uniquely conserved gene-expression profile in eosinophilic esophagitis. *J. Clin. Invest.* **116**, 536–547 (2006).
- Cork, M.J. *et al.* Epidermal barrier dysfunction in atopic dermatitis. *J. Invest. Dermatol.* **129**, 1892–1908 (2009).
- Prassas, I., Eissa, A., Poda, G. & Diamandis, E.P. Unleashing the therapeutic potential of human kallikrein-related serine proteases. *Nat. Rev. Drug Discov.* **14**, 183–202 (2015).
- Su, A.I. *et al.* A gene atlas of the mouse and human protein-encoding transcriptomes. *Proc. Natl. Acad. Sci. USA* **101**, 6062–6067 (2004).
- Wu, C. *et al.* BioGPS: an extensible and customizable portal for querying and organizing gene annotation resources. *Genome Biol.* **10**, R130 (2009).
- Sanderson, C.J. Interleukin-5, eosinophils, and disease. *Blood* **79**, 3101–3109 (1992).
- Shum, B.O. *et al.* The adipocyte fatty acid-binding protein aP2 is required in allergic airway inflammation. *J. Clin. Invest.* **116**, 2183–2192 (2006).
- Alevy, Y.G. *et al.* IL-13-induced airway mucus production is attenuated by MAPK13 inhibition. *J. Clin. Invest.* **122**, 4555–4568 (2012).
- Weirauch, M.T. *et al.* Determination and inference of eukaryotic transcription factor sequence specificity. *Cell* **158**, 1431–1443 (2014).
- Jiang, M. *et al.* BMP-driven NRF2 activation in esophageal basal cell differentiation and eosinophilic esophagitis. *J. Clin. Invest.* **125**, 1557–1568 (2015).
- Huang da, W., Sherman, B.T. & Lempicki, R.A. Systematic and integrative analysis of large gene lists using DAVID bioinformatics resources. *Nat. Protoc.* **4**, 44–57 (2009).
- Huang da, W., Sherman, B.T. & Lempicki, R.A. Bioinformatics enrichment tools: paths toward the comprehensive functional analysis of large gene lists. *Nucleic Acids Res.* **37**, 1–13 (2009).
- Potti, T.A., Petty, E.M. & Lesperance, M.M. A comprehensive review of reported heritable noggin-associated syndromes and proposed clinical utility of one broadly inclusive diagnostic term: NOG-related-symphalangism spectrum disorder (NOG-SSD). *Hum. Mutat.* **32**, 877–886 (2011).
- Miners, J.S., Renfrew, R., Swirski, M. & Love, S. Accumulation of alpha-synuclein in dementia with Lewy bodies is associated with decline in the alpha-synuclein-degrading enzymes kallikrein-6 and calpain-1. *Acta Neuropathol. Commun.* **2**, 164 (2014).
- Ota, T. *et al.* Complete sequencing and characterization of 21,243 full-length human cDNAs. *Nat. Genet.* **36**, 40–45 (2004).
- la Cour, T. *et al.* Analysis and prediction of leucine-rich nuclear export signals. *Protein Eng. Des. Sel.* **17**, 527–536 (2004).
- Kosugi, S., Hasebe, M., Tomita, M. & Yanagawa, H. Systematic identification of cell cycle-dependent yeast nucleocytoplasmic shuttling proteins by prediction of composite motifs. *Proc. Natl. Acad. Sci. USA* **106**, 10171–10176 (2009).
- Zhang, Y. I-TASSER server for protein 3D structure prediction. *BMC Bioinform.* **9**, 40 (2008).
- States, D.J. & Gish, W. Combined use of sequence similarity and codon bias for coding region identification. *J. Comput. Biol.* **1**, 39–50 (1994).
- Dickson, K.A., Haigis, M.C. & Raines, R.T. Ribonuclease inhibitor: structure and function. *Prog. Nucleic Acid Res. Mol. Biol.* **80**, 349–374. (05)80009-1 (2005).
- Wilmanski, J.M., Petnicki-Ocwieja, T. & Kobayashi, K.S. NLR proteins: integral members of innate immunity and mediators of inflammatory diseases. *J. Leukoc. Biol.* **83**, 13–30 (2008).
- McClure, R. & Massari, P. TLR-dependent human mucosal epithelial cell responses to microbial pathogens. *Front. Immunol.* **5**, 386 (2014).
- Wang, T. *et al.* Flightless I homolog negatively modulates the TLR pathway. *J. Immunol.* **176**, 1355–1362 (2006).
- Powell, S. *et al.* eggNOG v4.0: nested orthology inference across 3686 organisms. *Nucleic Acids Res.* **42**, D231–D239 (2014).
- Zimmermann, N. *et al.* Dissection of experimental asthma with DNA microarray analysis identifies arginase in asthma pathogenesis. *J. Clin. Invest.* **111**, 1863–1874 (2003).
- Langmead, B., Trapnell, C., Pop, M. & Salzberg, S.L. Ultrafast and memory-efficient alignment of short DNA sequences to the human genome. *Genome Biol.* **10**, R25 (2009).
- Trapnell, C. *et al.* Differential analysis of gene regulation at transcript resolution with RNA-seq. *Nat. Biotechnol.* **31**, 46–53 (2013).
- Garber, M., Grabherr, M.G., Guttman, M. & Trapnell, C. Computational methods for transcriptome annotation and quantification using RNA-seq. *Nat. Methods* **8**, 469–477 (2011).
- Pfaffl, M.W. A new mathematical model for relative quantification in real-time RT-PCR. *Nucleic Acids Res.* **29**, e45 (2001).
- Zuo, L. *et al.* IL-13 induces esophageal remodeling and gene expression by an eosinophil-independent, IL-13R alpha 2-inhibited pathway. *J. Immunol.* **185**, 660–669 (2010).
- Wen, T. *et al.* Molecular diagnosis of eosinophilic esophagitis by gene expression profiling. *Gastroenterology* **145**, 1289–1299 (2013).

42. Andl, C.D. *et al.* Epidermal growth factor receptor mediates increased cell proliferation, migration, and aggregation in esophageal keratinocytes in vitro and in vivo. *J. Biol. Chem.* **278**, 1824–1830 (2003).
43. Harada, H. *et al.* Telomerase induces immortalization of human esophageal keratinocytes without p16INK4a inactivation. *Mol. Cancer Res.* **1**, 729–738 (2003).
44. Oyama, K. *et al.* AKT induces senescence in primary esophageal epithelial cells but is permissive for differentiation as revealed in organotypic culture. *Oncogene* **26**, 2353–2364 (2007).
45. Wu, D. *et al.* Interleukin-13 (IL-13)/IL-13 receptor alpha1 (IL-13Ralpha1) signaling regulates intestinal epithelial cystic fibrosis transmembrane conductance regulator channel-dependent Cl<sup>-</sup> secretion. *J. Biol. Chem.* **286**, 13357–13369 (2011).